Earth and Planetary Science Letters 294 (2010) 223–229

Contents lists available at ScienceDirect

Earth and Planetary Science Letters

journal homepage: www.elsevier.com/locate/epsl

Planetary surface dating from crater size–frequency distribution measurements: Partial resurfacing events and statistical age uncertainty

G.G. Michael *, G. Neukum

Institute of Geological Sciences, Freie Universitaet Berlin, Malteser Strasse 74-100, Haus D, Berlin 12249, Germany

ARTICLE INFO

Article history:
Accepted 24 December 2009
Available online 1 February 2010

Keywords:
crater counting
surface dating
moon
Mars
resurfacing
age uncertainty

ABSTRACT

We describe the procedure to fit a cumulative production function polynomial to a partial crater size–frequency distribution. The technique is of particular use in deriving ages for surfaces which have undergone partial resurfacing events: namely, erosional or depositional events which have affected a limited diameter range of the crater population. We demonstrate its use in obtaining times for both the surface formation and the resurfacing event.

We give a practical outline of the method for making age measurements from crater counts and how to identify resurfacing effects in the results. We discuss the conversion of production function polynomials between common presentations, and the statistical uncertainty of the determined ages with respect to the non-linear chronology function, and a minor refinement of data binning.

1. Established surface dating method

The method of determining absolute ages for cratered planetary surface units has been described and developed in many papers (e.g. Hartmann et al., 1981; Neukum and Hiller, 1981; Neukum, 1983; Neukum and Ivanov, 1994; Hartmann and Neukum, 2001; Ivanov, 2001). The concept is to fit the observed crater size–frequency distribution (SFD) of a given surface unit to a known crater production function (PF), and to use the crater frequency for certain crater sizes together with a calibrating chronology function (CF) to obtain an absolute age.

The production function describes how many craters of a given size are formed in relation to the number of any other size. It is determined by considering the crater size–frequency distributions of homogeneous surface units of the Moon or Mars. Since the oldest units are best characterized in age by the larger range of crater sizes and younger units by lesser craters, to construct the production function for the entire observable diameter range it is necessary to use a piecewise normalization procedure. The function is plotted as a reverse-cumulative histogram on logarithmic scales, which is fitted with a polynomial approximation for use in the subsequent analysis (Fig. 1a).

The cumulative presentation has the advantage over the alternative incremental form of lower variability with statistical noise (Arvidson et al., 1979): for this reason we find it well-suited to the application of a fitting procedure from which we derive repeatable and intercomparable cratering model ages. In Section 4.1 we give the expression for the cumulative production function polynomials in differential form, so that the essence of the two most used chronology systems–their isochrons–can be directly compared, irrespective of presentation.

The radiometric dating of lunar rock samples permits an absolute calibration of the method (e.g. Hartmann et al., 1981; Neukum and Ivanov, 1994; Neukum et al., 2001). For known points on the surface we have crystallization ages, to which the measured crater populations of the containing units correspond. The relation can be approximated by a function which, in a cumulative form, describes a constant cratering rate going back to around 3 Ga, going over into an exponentially increasing rate beyond that time (Fig. 1b).

To measure the age of a lunar surface unit, one plots its cumulative crater size–frequency distribution normalised to a unit area, and shifts the production function in absolute crater frequency until it fits the data points. It is then possible to read off the cumulative frequency at a standard crater diameter (we use 1 km), and use that value to obtain a cratering model age from the chronology function. Alternatively, it is possible to construct the expected cumulative crater frequency for a given surface age—an isochron diagram (Fig. 1c).

Dating of other planetary surfaces requires a consideration of the cratering rate relative to that on the Moon (Neukum and Wise, 1976; Hartmann, 1977; Ivanov, 2001; Hartmann and Neukum, 2001; Neukum et al., 2001). The essential elements of this consideration are: the relative impactor flux and its velocity distribution, derived from the observed distribution of asteroidal orbits; the produced crater size as a function of impactor size, taking account of the changed velocity distribution, gravity conditions and target properties; and a

* Corresponding author.
E-mail addresses: gregory.michael@fu-berlin.de (G.G. Michael), gerhard.neukuml@fu-berlin.de (G. Neukum).

0012-821X/$ – see front matter © 2010 Elsevier B.V. All rights reserved.
doi:10.1016/j.epsl.2009.12.041

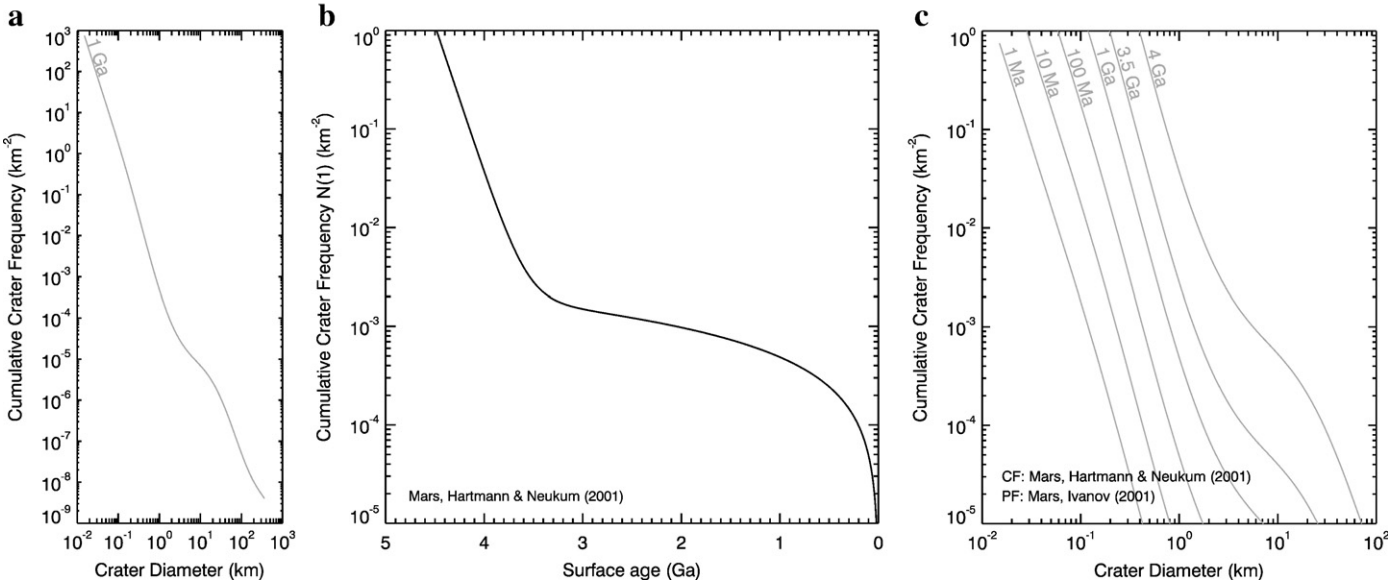

Fig. 1. a: Polynomial derived from piecewise-normalised production function (Neukum, 1983; Neukum and Ivanov, 1994; Ivanov, 2001). b: Mars chronology function (Hartmann and Neukum, 2001; Ivanov, 2001; Neukum et al., 2001). c: Mars cumulative crater frequency isochrons: the Mars production function plotted to intersect cumulative frequency values at $D=1$ km for a series of ages (marked). Cumulative frequency values taken from the chronology function.

normalization with respect to the collisional cross-section and the planets' surface area.

The production functions for the Moon and Mars are shown in *R*-plot form in Fig. 4 (see later for additional details about the *R*-plot). The extrema in the curves are characteristic of the size–frequency distribution of the impactor population. One may note the shift of the inflexions towards lower crater diameters when going from the Moon to Mars, which is largely a consequence of the lesser impact velocities at Mars, as well as the shift towards higher surface density, resulting from the increased impactor flux at Mars.

2. Resurfacing

Erosional or mantling resurfacing processes typically change the crater population by removing members from the low-diameter end of the distribution. Craters of lesser diameter having less topographic expression, or less displaced mass relative to an evensurface, are expected to be preferentially obliterated by any resurfacing process (Hartmann, 1971; Neukum and Horn, 1976; Neukum and Hiller, 1981; Hartmann and Werner, 2010-this issue).

If we have a surface which formed at time t_0, and such a resurfacing process occurs for a period up to a time t_1 removing all craters with a diameter below D_1, at a later time of observation, we expect to observe a crater population which reflects the age t_0 for craters of diameter $D>D_1$ and the age t_1 for craters with $D<D_1$.

On a differential crater frequency plot, the effect on the distribution is seen directly as a diminished low-diameter end of the distribution. On a cumulative crater frequency (N_{cum}) plot, which plots the number of craters exceeding diameter D per unit area, it appears as a step in the distribution between two segments which have different tangential isochrons (Fig. 2a). The lower isochron can be used to make a first order estimate of the time of end of the resurfacing event t_1 (as done by Neukum and Hiller, 1981), but the cumulative plot in this region includes the larger craters which were formed between t_0 and t_1 causing an overestimate of t_1. The degree of the overestimate depends on the difference between t_0 and t_1 as well as the slope of the step: a step occurring over a narrow diameter range has a larger effect.

One approach to this problem is to estimate the excess crater population above the step diameter for the difference in ages between the older and younger isochrons, and subtract this value from the cumulative population before fitting a more precise isochron (Werner, 2005). This solution requires the estimation of four parameters to describe two diameter ranges: one range for the older isochron, and one for the sought younger isochron. However, since a surface age can be determined from any subset ofthe diameter range of an undisturbed crater population, it follows that the calculation may be made without referral to the older isochron, and therefore using only two parameters (Michael and Neukum, 2007). This necessarily increases the precision and repeatability of the results. We estimate the larger population as it would appear if it matched the age of the younger segment of the distribution by iterative fitting of the production function, improving the estimate at each step.

When we can assume that a portion of the size–frequency distribution represents a single age–namely, the time since the finish of a resurfacing event–we have a set of cumulative values, $N_{cum}(D)$, which are all in error by an unknown offset k. The last value of the range, $N_{cum}(D_{max})$, represents the density of craters too large to be influenced by the resurfacing, which is unknown. The effect of k, if positive, is to decrease the gradient of the cumulative plot over the range of interest relative to the known production function; when negative, to increase it. By fitting (in a least squares sense) the production function to the given range of N_{cum} and using the resultant curve to obtain a new estimate for $N_{cum}(D_{max})$ and hence k, one can obtain the value of k which gives the best fit to the production curve within a few iterations. The corrected values of $N_{cum}(D)$ can then be used in the usual manner to obtain a time estimate for the end of the resurfacing event.

Fig. 2a shows a crater count from Echus Chasma, Mars, channel unit Ar1A (Neukum et al., 2010-this volume) illustrating a partial resurfacing event. The larger craters of the distribution lie on the 3.69 Ga isochron. Towards lesser diameters, the distribution flattens and then increases in slope, finally almost to follow the 1.05 Ga isochron. The interpretation of the plot is that after the surface was formed 3.69 Ga ago, the crater population was building up in accordance with the production function until some surface process began which reduced the population of craters below 600 m in diameter, and likely wholly removed the population of craters below 250 m in diameter. This process, of unknown duration, had ceased by a time around 1 Ga ago, after which the population in the size

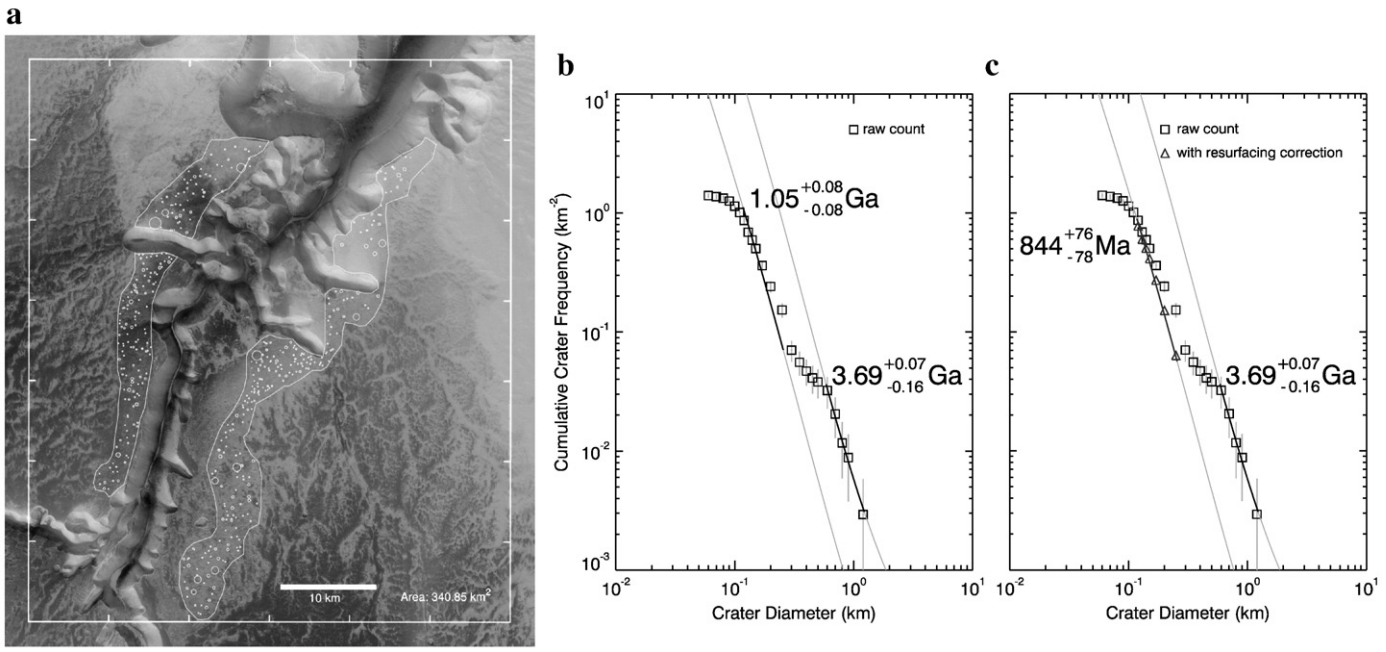

Fig. 2. Marked crater count of unit Ar1A of Echus Chasma (HRSC image 2204_0000, Neukum et al., 2010-this volume). a: Cumulative crater frequency plot showing production function fitted to the crater diameter range 0.6–1.2 km, and the model age, 3.69 Ga, taken from the chronology function for the frequency value at $D = 1$ km. A similar fit is attempted for the range 120–250 m and an age estimate of 1.05 Ga made, but we see the points lie on a shallower curve than the PF. b: The range 120–250 m corrected for resurfacing (triangles): the excess of older craters in the cumulative curve above 250 m is removed, and a corrected model age of 844 Ma is found. Error bars are $\pm\frac{1}{Area}[N_{cum}(D)]^{1/2}$ c: Echus Chasma Unit Ar1A. The boundary of the counting area and the measured craters are marked.

range less than 250 m diameter began to build up once more in accordance with the production function. It should be noted that the fall-off at the smallest diameters (100 m and less) is a consequence of the resolution limitof the image used to make the crater counts, and is a commonly observed effect.

The slope of the upper steep section is somewhat less than the 1.05 Ga isochron shown: this is a consequence of the excess craters in the cumulative crater frequency values deriving from the older portion of the distribution. Fig. 2b shows the portion of the distribution judged to correspond to this younger isochron corrected by the method described above (triangular symbols). The excess is eliminated from the cumulative values in such a way as to give a best match to the isochron slope, after which a corrected model age of 844 Ma is found.

On an ideal accumulating surface, i.e. one with no resurfacing history, the theoretical size–frequency distribution over all diameters is fixed by knowledge of the distribution over any limited range, since the production function describes the relative abundances outside that range. Real counts on younger surfaces are often observed to correspond to the production function over their full diameter range, aside from the resolution fall-off at low diameters. Older surface units have commonly experienced resurfacing to some extent, and the characteristic 'kink' between two portions of the SFD corresponding to different isochrons is often seen. In such a case, we can apply the resurfacing correction method to find ages for each portion of the distribution: the older corresponding to the formation of the surface; the younger to the end of the action of the resurfacing process.

However, as may be expected, many old surfaces have a more complex history: in general, they may have experienced varying resurfacing over time, producing a cumulative SFD which falls beneath the PF towards lower diameters in a continuously variable manner. In some cases it may be possible to interpret more than one resurfacing event; in others there may be no distinct events, but nevertheless the craters falling within any given size-band may be related to a characteristic time, earlier than which they were not being accumulated.

The technique has already been applied in several works (e.g. Williams et al., 2008; Neukum et al., 2010-this volume).

3. Method

This section gives a brief account of the steps involved in dating a surface unit.

3.1. Mapping

It only makes sense to attempt to assess the age of a surface which has a uniform history. Practically, this means mapping the outline of a geologically homogeneous region that is interpreted to have undergone spatially uniform geologic processes. Significant interruptions to the homogeneity should be excluded from the mapped area, as should areas with steep slopes where craters do not accumulate at the same rate (Basilevsky, 1976), and areas with identifiable secondary cratering. Crater clusters from a fragmented impactor should normally also be excluded from the counting area.

3.2. Crater counting

Normally, every identifiable impact crater whose centre lies within the mapped region should be measured. In special cases, such as the dating of a thin superposed layer where one would measure only the superposed craters, the criteria for inclusion may be different. It should be ensured that the technique used to measure the crater diameters takes account of the varying map scale across the image according to its map projection.

One should be careful to identify only impact craters: there are other common features, such as collapse pits, sublimation pits and volcanic calderas which, particularly when close to the resolution limit, might be mistaken for impact features. Secondary craters, where recognisable as clusters or chains, should be excluded together with the vicinity they occupy (the issue of secondary

cratering is discussed at length in McEwen and Bierhaus, 2006; Dundas and McEwen, 2007; Hartmann, 2007; Werner et al., 2009; Neukum et al., 2010-this volume).

3.3. How to select fitting range

Having a complete list of crater diameters and a value for the area over which they were counted, one can construct a log N_{cum} vs. log D and attempt to find the isochron which best fits the data (Fig. 1c). In typical cases, a range of the data points on the large diameter end will lie along a single isochron before they begin to fall beneath it at smaller diameters.

To find the base age for the surface, i.e. the time before which craters were not being accumulated, one should shift the production function curve up or down to fit this range of data points.

3.4. When to use the resurfacing correction

The fall-off in N_{cum} towards lower diameters may have several causes. One is a data effect: approaching the resolution limit of the image it becomes harder to identify smaller craters with the result that fewer are counted, although they may exist on the surface. This produces a characteristic roll-off, which is seen in nearly every complete count. In Fig. 2a it can be seen in the portion of the curve representing craters smaller than 100 m. If the count is supplemented with another from higher resolution imagery, the effect is removed (although it will occur again at a smaller diameter).

The second cause is a real one: some resurfacing process, preferentially removing craters from the low-diameter edge of the size distribution. The shape of the fall-off may vary, depending on the time-extent and intensity of the process. In some cases, the N_{cum} curve is seen to fall beneath the base age isochron and then resteepen to nearly parallel a younger isochron: in such a case it is appropriate to use the resurfacing correction described earlier. To do so requires a judgement of the diameter range representing the crater population after the end of the resurfacing stage: this should be the portion of the curve which nearly parallels the younger isochron before any additional fall-off occurs (either because of the resolution rollover or later resurfacing).

In the example of Fig. 2a this range is 120 m to 250 m. After the correction, the points are seen to lie close to a single isochron, on a somewhat steeper curve than before. That they do lie well on the isochron is a confirmation that the diameter range was correctly chosen.

It should be noted that a reduction in the steepness of the distribution is also seen when the surface reaches saturation equilibrium towards lesser diameters: this can be distinguished from resurfacing by its occurrence at a known crater density (Gault, 1970; Hartmann, 1984). In this case no resteepening is observed.

3.5. Problematic curves

Occasionally, an N_{cum} curve is seen to deviate over some diameter interval above the isochron established at larger diameters. Assuming the count is complete, this is an indication of clustering in the area: a closer inspection of the surface will normally show that the spatial distribution of the craters in this size range is not random, and that at least some of them were not formed independently: either the result of single-event fragmented impacts, or secondary craters not identified before counting. Such clusters should have been excluded from the counting area.

4. Differential forms of production function polynomials

Since the production function is a simple curve on a log N_{cum} vs. log D plot, it was found convenient to approximate this with a polynomial function (Neukum, 1983; Neukum and Ivanov, 1994; Ivanov, 2001)

$$logN_{cum} = p, \text{ where } p = \sum_{i=0}^{n} a_i x^i \text{ and } x = logD.$$

It can be useful to express this function in a differential form,

$$F = -\frac{dN}{dD} = -\frac{dN}{dp}\cdot\frac{dp}{dx}\cdot\frac{dx}{dD} \quad (1)$$

$$= -10^p ln10 \cdot \sum_{j=1}^{n} j a_j x^{j-1} \cdot \frac{1}{Dln10} \quad (2)$$

$$= -\frac{1}{D}\cdot 10^{\sum_{i=0}^{n} a_i x^i} \cdot \sum_{j=1}^{n} j a_j x^{j-1} \quad (3)$$

so as to be able to make a direct comparison with the isochrons used in the Hartmann presentation, or for considerations in connection with transforming the function between the Moon and other bodies.

4.1. Hartmann presentation

In the Hartmann presentation, which is non-cumulative, the data are split into bins of width $D(\sqrt{2}-1)$, so the production function takes the form:

$$H(D) = FD(\sqrt{2}-1) \quad (4)$$

$$= -(\sqrt{2}-1)10^{\sum_{i=0}^{n} a_i x^i} \cdot \sum_{j=1}^{n} j a_j x^{j-1} \quad (5)$$

Fig. 3 compares the Hartmann isochrons for Mars (2002 iteration, unpublished) with their equivalents derived from the Ivanov (2001) production function and the Hartmann and Neukum (2001) chronology. The Hartmann values are essentially the same for diameters below 1 km; they exceed those of the Ivanov production function by around a factor of 3 in the diameter range of 2–8 km; agree again over

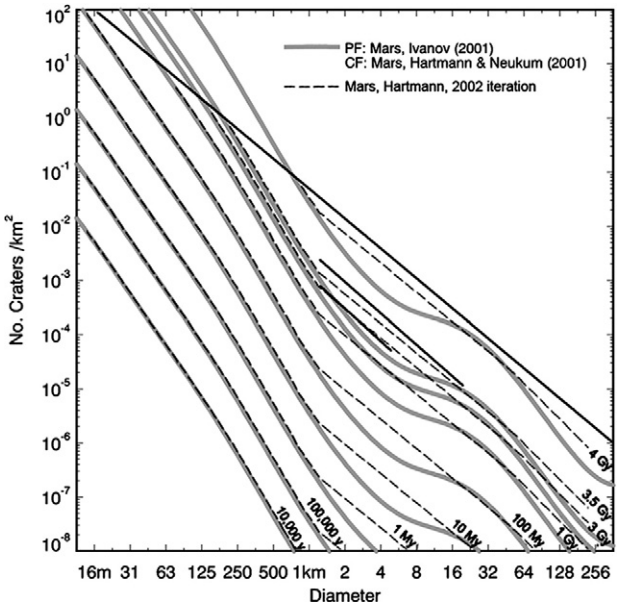

Fig. 3. Hartmann isochrons for Mars (2002 iteration, unpublished) with their equivalents derived from the Ivanov (2001) production function and the Hartmann and Neukum (2001) chronology. Solid black lines mark the saturation equilibrium, and Noachian–Hesperian and Hesperian–Amazonian boundaries.

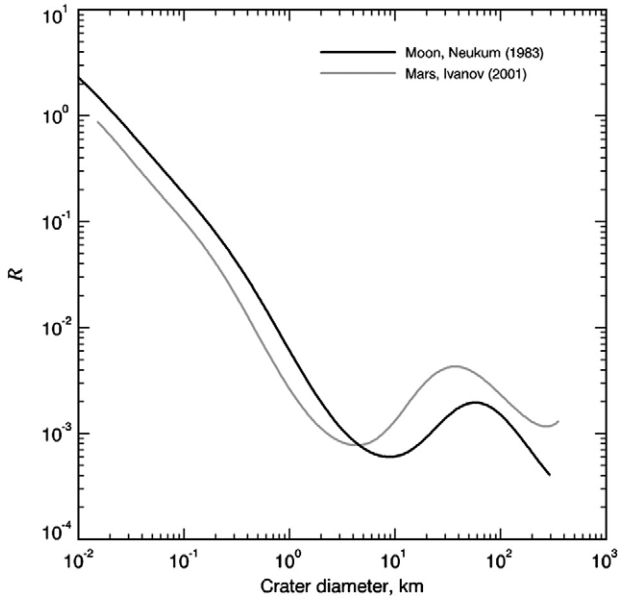

Fig. 4. *R*-curves for the lunar (Neukum, 1983) and Mars (Ivanov, 2001) production functions, for $t=2$ Ga. Note the shift of the extrema towards lower crater diameters when going from the Moon to Mars, which is largely a consequence of the lesser impact velocities at Mars, as well as the shift towards higher surface density, resulting from the increased impactor flux at Mars.

the range 16–64 km; and are greater by a factor of ~2 at the 256 km bin.

4.2. R-plot form

The *R*-plot (Arvidson et al., 1979) is the size–frequency distribution relative to a standard function, SD^{-3}. The standard function S is a first order approximation to the observed crater populations, and this relative form permits the more subtle deviations from this distribution to be emphasised. R is defined as

$$R(D) \equiv F(D) / S(D)$$

and so can be plotted from the polynomial production function as

$$R(D) = -D^2 10^{\sum_{i=0}^{n} a_i x^i} \cdot \sum_{j=1}^{n} j a_j x^{j-1}$$

The *R*-curves for the lunar (Neukum, 1983) and Mars (Ivanov, 2001) production functions are given in Fig. 4.

5. Non-binning of largest craters

The base age for a unit is typically strongly influenced by the large diameter tail of the size–frequency distribution. Since these bins contain the fewest craters, there can be a small loss of information by plotting them against the bin centre diameter. In the cumulative presentation, one may equivalently plot N_{cum} as a continuous function of D to retain this size information (it may be noted that the equivalent is not possible in a non-cumulative histogram). In practice this influences only the larger diameter bins, so for simplicity of presentation–i.e., not to overcrowd the plot with data points–may be combined with a binning for lower diameters.

6. Statistical age uncertainty

It should be emphasised that the uncertainty discussed in this section is that arising from the statistics of the Poisson cratering process tied to the non-linear chronology function of the model: the uncertainty within an individual cratering model age measurement. For a discussion of the *systematic* error of the model, which arises from uncertainties in the production and chronology functions and their interaction and, most importantly for Mars, from assumptions made about the relative impactor flux at its orbital position by comparison with that of the Moon, see Neukum et al. (2010-this volume). The statistical error determines how precisely one age measurement may be related to another: how certain, for example, that a surface unit measured to be 800 Ma is older than its neighbour measured at 750 Ma. Systematic errors relate to the absolute calibration of the model, and determine how closely the crater model ages relate to the true time-scale of the Solar System.

It is sometimes asked what minimum area should be counted to achieve a good age measurement, but it is rather the number of observed craters relevant to the age measurement which determines its precision. The area required to accumulate this number depends itself on the age of the surface. Younger surfaces are typically dated from smaller diameter craters which occur with higher areal density; it can be sufficient to count craters over a smaller area, although at higher image resolution. Older surfaces are dated from the larger craters which occur over larger areas, where a lower image resolution may suffice.

The occurrence of craters on an accumulating surface, caused by independently arriving impactors, is described by a Poisson distribution. The probability of observing k accumulated craters is given by the equation

$$p = \frac{\lambda^k e^{-\lambda}}{k!}$$

where λ is the expected number of impacts in the time interval t, the measured age of the surface. The observation of k is already a measurement of the most likely value of λ, but the equation determines the probability of λ taking any other value: in other words, the likelihood that the surface shows a different number of craters from that which would be expected for its true age, t'. Variations of λ correspond proportionally to those of N_{cum} (1), which relates to the age through the chronology function. Thus one can construct a plot of probability density vs. age t' for any given k and N_{cum} (1). The consideration here, as those which have assumed a $1/\sqrt{N}$ standard deviation previously, assumes all the impactors to be governed by the same λ. This is not strictly correct, since λ is a function of crater diameter, but an adequate approximation to reveal the general character of the statistical age uncertainty.

Fig. 5 shows the statistical age uncertainty curves for measurements on surfaces with various measured ages, t, based on differing numbers, k, of observed craters using the Hartmann and Neukum (2001) chronology function. The curves can be read as the probability of the surface having an age other than the nominal measured value. For $t=0.5$ Ga the curves for $k=1$, 3, 5, 8, 13 craters show the progression from the asymmetrical shape characteristic of the Poisson distribution at low k towards a more Gaussian-like form at higher k. For $t=2$ Ga, the spread of the distribution is increased proportionately for equivalent k; to achieve a comparable precision in absolute terms requires markedly more craters (compare the curve for 8 craters at 0.5 Ga with that for 89 at 2 Ga). Beyond 3 Ga, the exponential term of the chronology function becomes significant, expressing the increasing cratering rate before this time. Its effect is to compress the uncertainty curves laterally rather strongly with the consequence that the number of craters required for a given absolute precision once more falls. In the plot shown for $t=3$ Ga, this compression is seen in the right wings of the distributions by comparison with those for $t=2$ Ga. At $t=3.6$ Ga, a roughly equivalent absolute precision is achieved for a measurement with $k=5$ craters (compared again to the curve for 8 craters at 0.5 Ga and that for 89 at 2 Ga).

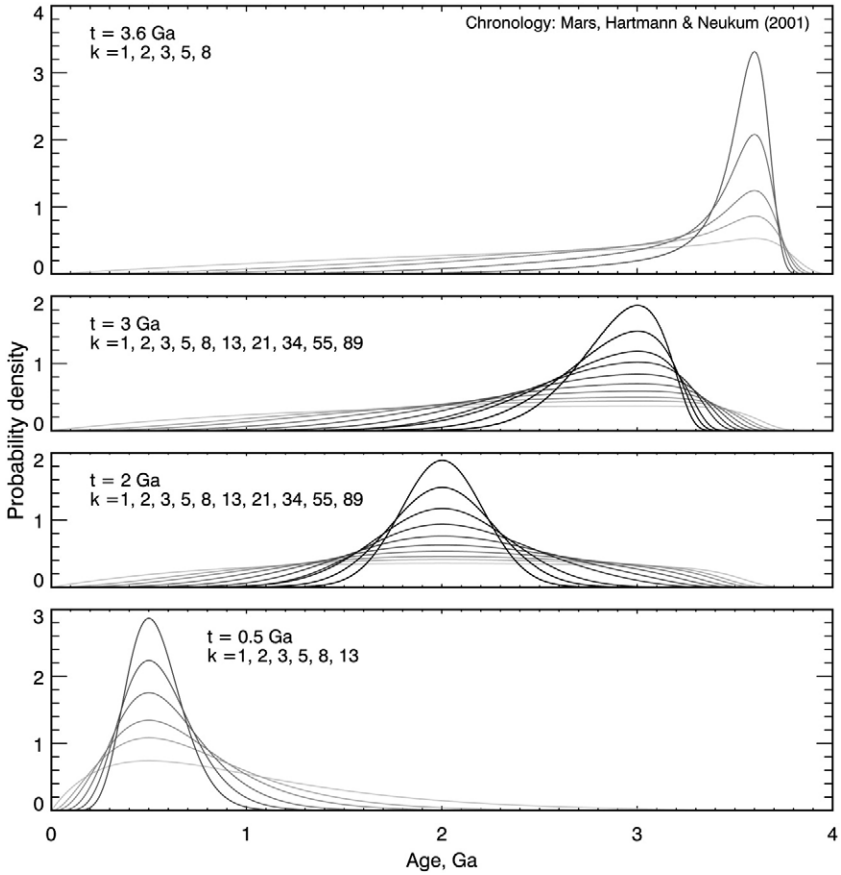

Fig. 5. Statistical age uncertainty curves for measured ages, $t = 0.5, 2, 3, 3.6$ Ga, with varying number of counted craters, k, based upon the Hartmann and Neukum (2001) chronology function. The curves can be interpreted as the probability of the surface having an age other than the nominal measured value.

7. Software

A software tool named craterstats, developed by the first author to derive ages from crater counts as described in this paper, is available for others to use from http://hrscview.fu-berlin.de/software.html.

Acknowledgements

This research was partly supported by the German Science Foundation (DFG) through the Priority Program "Mars and the Terrestrial Planets" (DFG-SPP 1115, Project: Chronostratigraphy of Mars, grant: NE 212/8-3), by the Helmholtz Association through the research alliance "Planetary Evolution and Life", and by the German Space Agency (DLR), grant: 50QM0301 (HRSC on Mars Express).

References

Arvidson, R.E., Boyce, J., Chapman, C., Cintala, M., Fulchignoni, M., Moore, H., Neukum, G., Schultz, P., Soderblom, L., Strom, R., Woronow, A., Young, R., 1979. Standard techniques for presentation and analysis of crater size–frequency data. Icarus 37, 467–474. doi:10.1016/0019-1035(79)90009-5 February.

Basilevsky, A.T., 1976. On the rate of evolution of small lunar craters. Lunar and Planetary Institute Science Conference Abstracts, volume 7 of Lunar and Planetary Inst. Technical Report, pp. 32–34. March.

Dundas, C.M., McEwen, A.S., 2007. Rays and secondary craters of Tycho. Icarus 186, 31–40. doi:10.1016/j.icarus.2006.08.011 January.

Gault, D.E., 1970. Saturation and equilibrium conditions for impact cratering on the lunar surface: criteria and implications. Radio Sci. 5, 273–291. doi:10.1029/RS005i002p00273 February.

Hartmann, W.K., 1971. Martian cratering III: theory of crater obliteration. Icarus 15, 410–428. doi:10.1016/0019-1035(71)90119-9 December.

Hartmann, W.K., 1977. Relative crater production rates on planets. Icarus 31, 260–276. doi:10.1016/0019-1035(77)90037-9 June.

Hartmann, W.K., 1984. Does crater 'saturation equilibrium' occur in the solar system? Icarus 60, 56–74. doi:10.1016/0019-1035(84)90138-6 October.

Hartmann, W.K., 2007. Martian cratering 9: toward resolution of the controversy about small craters. Icarus 189, 274–278. doi:10.1016/j.icarus.2007.02.011 July.

Hartmann, W.K., Neukum, G., 2001. Cratering chronology and the evolution of Mars. Space Sci. Rev. 96, 65–194 April.

Hartmann, W.K., Werner, S.C., 2010. Martian cratering 10. Progress in use of crater counts to interpret geological processes: Examples from two debris aprons. Earth Planet. Sci. Lett. 294, 230–237 (this issue).

Hartmann, W.K., Strom, R.G., Weidenschilling, S.J., Blasius, K.R., Voronow, A., Dence, M.R., Grieve, R.A.F., Diaz, J., Chapman, C.R., Shoemaker, E.M., Jones, K.L., 1981. Basaltic Volcanism on the Terrestrial Planets. Pergamon Press Inc, New York.

Ivanov, B.A., 2001. Mars/moon cratering rate ratio estimates. Space Sci. Rev. 96, 87–104 April.

McEwen, A.S., Bierhaus, E.B., 2006. The importance of secondary cratering to age constraints on planetary surfaces. Annu. Rev. Earth Planet. Sci. 34, 535–567. doi:10.1146/annurev.earth.34.031405.125018 May.

Michael, G., Neukum, G., 2007. Refinement of cratering model age for the case of partial resurfacing. Lunar and Planetary Institute Science Conference Abstracts, volume 38 of Lunar and Planetary Inst. Technical Report, pp. 1825–1826. March.

Neukum, G, Meteoritenbombardement und Datierung planetarer Oberflachen. Habilitation, University of Munich, February 1983.

Neukum, G. and Hiller, K. Martian ages. J. Geophys. Res. 86, 3097–3121, April 1981. doi:10.1029/JB086iB04p03097.

Neukum, G., Horn, P., 1976. Effects of lava flows on lunar crater populations. Moon 15, 205–222. doi:10.1007/BF00562238 July.

Neukum, G., Ivanov, B.A., 1994. Crater size distributions and impact probabilities on Earth from lunar, terrestrial-planet, and asteroid cratering data. In: Gehrels, T., Matthews, M.S., Schumann, A.M. (Eds.), Hazards Due to Comets and Asteroids, pp. 359–416.

Neukum, G., Wise, D.U., 1976. Mars — a standard crater curve and possible new time scale. Science 194, 1381–1387. doi:10.1126/science.194.4272.1381 December.

Neukum, G., Ivanov, B.A., Hartmann, W.K., 2001. Cratering records in the inner solar system in relation to the lunar reference system. Space Sci. Rev. 96, 55–86 April.

Neukum, G., Basilevsky, A.T., Kneissl, T., Chapman, M.G., van Gasselt, S., Michael, G., Jaumann, R., Hoffmann, H., Lanz, J., 2010. The geologic evolution of Mars: Episodicity of resurfacing events and ages from cratering analysis of image data

and correlation with radiometric ages of Martian meteorites. Earth Planet. Sci. Lett. 294, 204–222 (this issue).
Werner, S.C. Major Aspects of the Chronostratigraphy and Geologic Evolutionary History of Mars. PhD thesis, Freie Universitaet Berlin, December 2005.
Werner, S.C., Ivanov, B.A., Neukum, G., 2009. Theoretical analysis of secondary cratering on Mars and an image-based study on the Cerberus Plains. Icarus 200, 406–417. doi:10.1016/j.icarus.2008.10.011 April.
Williams, D.A., Greeley, R., Werner, S.C., Michael, G., Crown, D.A., Neukum, G., Raitala, J., 2008. Tyrrhena Patera: geologic history derived from Mars express high resolution stereo camera. J. Geophys. Res. (Planets) 113 (12), 11005-+. doi:10.1029/2008JE003104 November.